VOLUME 101 | SUPPLEMENT 1 | MARCH 2021

LI LABORATORY INVESTIGATION

THE BASIC AND TRANSLATIONAL PATHOLOGY RESEARCH JOURNAL

ABSTRACTS

MEDICAL RENAL PATHOLOGY
(INCLUDING RENAL TRANSPLANTATION)
(828-847)

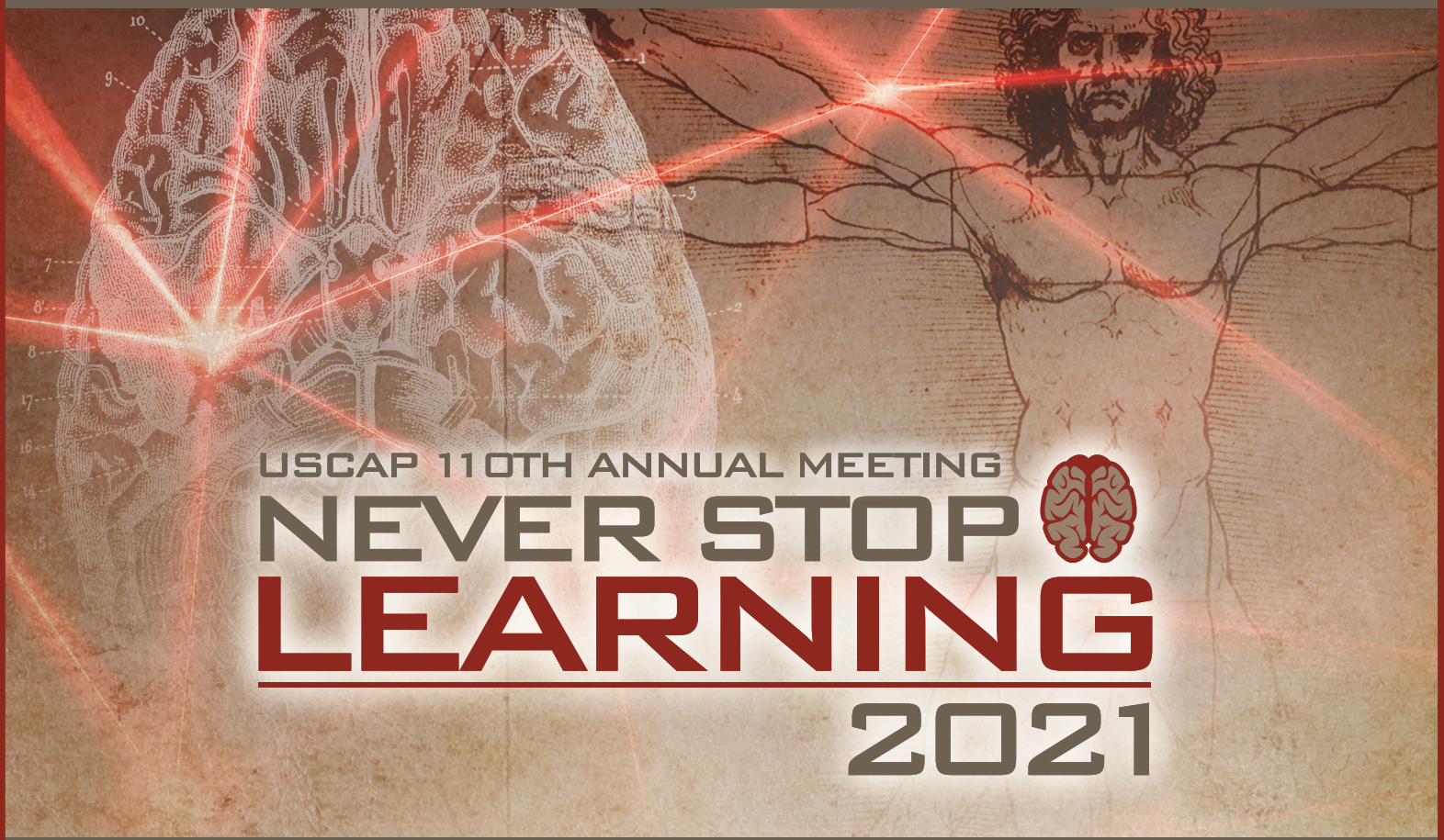

MARCH 13-18, 2021 | VIRTUAL AND INTERACTIVE

Published by
SPRINGER NATURE
www.ModernPathology.org

USCAP
Creating a Better Pathologist
AN OFFICIAL JOURNAL OF THE UNITED STATES AND CANADIAN ACADEMY OF PATHOLOGY

EDUCATION COMMITTEE

Jason L. Hornick
Chair

Rhonda K. Yantiss, Chair
Abstract Review Board and Assignment Committee

Kristin C. Jensen
Chair, CME Subcommittee

Laura C. Collins
Interactive Microscopy Subcommittee

Raja R. Seethala
Short Course Coordinator

Ilan Weinreb
Subcommittee for Unique Live Course Offerings

David B. Kaminsky
(Ex-Officio)
Zubair W. Baloch
Daniel J. Brat
Sarah M. Dry
William C. Faquin
Yuri Fedoriw
Karen Fritchie
Jennifer B. Gordetsky
Melinda Lerwill
Anna Marie Mulligan
Liron Pantanowitz
David Papke,
Pathologist-in-Training
Carlos Parra-Herran
Rajiv M. Patel
Deepa T. Patil
Charles Matthew Quick
Lynette M. Sholl
Olga K. Weinberg
Maria Westerhoff
Nicholas A. Zoumberos,
Pathologist-in-Training

ABSTRACT REVIEW BOARD

Benjamin Adam
Rouba Ali-Fehmi
Daniela Allende
Ghassan Allo
Isabel Alvarado-Cabrero
Catalina Amador
Tatjana Antic
Roberto Barrios
Rohit Bhargava
Luiz Blanco
Jennifer Boland
Alain Borczuk
Elena Brachtel
Marilyn Bui
Eric Burks
Shelley Caltharp
Wenqing (Wendy) Cao
Barbara Centeno
Joanna Chan
Jennifer Chapman
Yunn-Yi Chen
Hui Chen
Wei Chen
Sarah Chiang
Nicole Cipriani
Beth Clark
Alejandro Contreras
Claudiu Cotta
Jennifer Cotter
Sonika Dahiya
Farbod Darvishian
Jessica Davis
Heather Dawson
Elizabeth Demicco
Katie Dennis
Anand Dighe
Suzanne Dintzis
Michelle Downes
Charles Eberhart
Andrew Evans
Julie Fanburg-Smith
Michael Feely
Dennis Firchau
Gregory Fishbein
Andrew Folpe
Larissa Furtado
Billie Fyfe-Kirschner
Giovanna Giannico
Christopher Giffith
Anthony Gill
Paula Ginter
Tamar Giorgadze
Purva Gopal
Abha Goyal
Rondell Graham
Alejandro Gru
Nilesh Gupta
Mamta Gupta
Gillian Hale
Suntrea Hammer
Malini Harigopal
Douglas Hartman
Kammi Henriksen
John Higgins
Mai Hoang
Aaron Huber
Doina Ivan
Wei Jiang
Vickie Jo
Dan Jones
Kirk Jones
Neerja Kambham
Dipti Karamchandani
Nora Katabi
Darcy Kerr
Francesca Khani
Joseph Khoury
Rebecca King
Veronica Klepeis
Christian Kunder
Steven Lagana
Keith Lai
Michael Lee
Cheng-Han Lee
Madelyn Lew
Faqian Li
Ying Li
Haiyan Liu
Xiuli Liu
Lesley Lomo
Tamara Lotan
Sebastian Lucas
Anthony Magliocco
Kruti Maniar
Brock Martin
Emily Mason
David McClintock
Anne Mills
Richard Mitchell
Neda Moatamed
Sara Monaco
Atis Muehlenbachs
Bita Naini
Dianna Ng
Tony Ng
Michiya Nishino
Scott Owens
Jacqueline Parai
Avani Pendse
Peter Pytel
Stephen Raab
Stanley Radio
Emad Rakha
Robyn Reed
Michelle Reid
Natasha Rekhtman
Jordan Reynolds
Andres Roma
Lisa Rooper
Avi Rosenberg
Esther (Diana) Rossi
Souzan Sanati
Gabriel Sica
Alexa Siddon
Deepika Sirohi
Kalliopi Siziopikou
Maxwell Smith
Adrian Suarez
Sara Szabo
Julie Teruya-Feldstein
Khin Thway
Rashmi Tondon
Jose Torrealba
Gary Tozbikian
Andrew Turk
Evi Vakiani
Christopher VandenBussche
Paul VanderLaan
Hannah Wen
Sara Wobker
Kristy Wolniak
Shaofeng Yan
Huihui Ye
Yunshin Yeh
Anjana Yeldandi
Gloria Young
Lei Zhao
Minghao Zhong
Yaolin Zhou
Hongfa Zhu

To cite abstracts in this publication, please use the following format: **Author A, Author B, Author C, et al. Abstract title (abs#). In "File Title."** ***Laboratory Investigation*** **2021; 101 (suppl 1): page#**

828 Endocarditis Associated Glomerulonephritis: A Series of 26 Cases from a Single Institution

Emad Ababneh[1], Leal Herlitz[2], Jane Nguyen[2]
[1]*Cleveland Clinic Foundation, Cleveland, OH,* [2]*Cleveland Clinic, Cleveland, OH*

Disclosures: Emad Ababneh: None; Leal Herlitz: None; Jane Nguyen: None

Background: Endocarditis – associated glomerulonephritis (ECGN) is a well-documented entity, yet clinically under-recognized due to overlapping features with other glomerulonephritides and occasional subacute onset at presentation. This study aimed to analyze clinical and pathologic characteristics of patients with ECGN.

Design: All cases with biopsy-proven ECGN in the period 2010-2019 were included. Clinical features were recorded and pathologic features were reviewed.

Results: 26 cases were identified, all presented with acute kidney injury (AKI). Mean patients' age was 51 years with M:F ratio of 3.3:1. The mean serum creatinine at presentation was 4.4 mg/dl. On urine dipstick, 88% and 85% of patients showed at least 2+ hematuria and 1+ proteinuria, respectively.13/24 patients showed hypocomplementemia and 8/24 demonstrated positive ANCA antibodies. Cryoglobulins were positive in 15 out of 18 patients tested. Data on the associated bacterial microorganism was present in 23 cases and showed *Staphylococcus aureus* (11), *Bartonella* (5), *Streptococcus viridans* (2), *Streptococcus mutans* (2), *Staphylococcus epidermidis* (1), *Streptococcus mitis-oralis* (1), *Enterococcus faecium* (1), and *Gemella* (1). 9/13 patients with hypocomplementemia and 7/8 of patients with ANCA antibodies were associated with non – *Staphylococcus* species including all cases of *Bartonella*. Light microscopy showed focal or diffuse endocapillary proliferative features in 81% of the cases. 77% of cases showed at least focal necrotizing crescent formation. An active tubulointerstitial infiltrate was seen in 77% of the cases. No cases showed arteritis. Immunofluorescence revealed dominant or co-dominant C3 staining (18/26 cases) and IgM was the most commonly deposited immunoglobulin with polyclonal 2-3+ staining in 32% of cases, followed by IgA in 20% of cases, while IgG was deposited (2-3+) only in 3 cases. Strong IgM staining was associated with all cases of *Bartonella* (5). Treatment included long-term antibiotics (24/24), heart valve repair/replacement (11/24), immunosuppression (4/24), and dialysis (5/24).

Conclusions: ECGN most commonly presents with AKI. In subacute endocarditis, positive ANCA serologies, and biopsy findings of crescentic GN can lead to a missed diagnosis. Strong staining for IgM as well as C3 was seen in cases of ECGN associated with *Bartonella* and other subacute organisms. A high index of suspicion was important for timely diagnosis as *Bartonella* is not detectable on routine blood culture.

829 Membranous Nephropathy with Tubular Basement Membrane Immune Deposits Following Stem Cell Transplant

Shahad Abdulameer[1], Kelly Smith[1], Charles Alpers[2], Megan Troxell[3]
[1]*University of Washington, Seattle, WA,* [2]*University of Washington School of Medicine, Seattle, WA,* [3]*Stanford University Medical Center, Stanford, CA*

Disclosures: Shahad Abdulameer: None; Kelly Smith: None; Charles Alpers: None; Megan Troxell: None

Background: A broad spectrum of kidney disorders following hematopoietic stem cell transplant (HSCT) is well documented in the literature. Common renal manifestations include membranous nephropathy, minimal change disease, collapsing glomerulopathy, graft versus host disease (GHVD) and thrombotic microangiopathy. We characterize the unique presentation of membranous nephropathy with concomitant tubular basement membrane deposits in this population.

Design: A 10-year (2011-2020) retrospective cohort study was conducted at two institutions using the following search criteria (bone marrow and peripheral blood stem cells transplant, kidney biopsy, proteinuria, membranous nephropathy, and tubular basement membrane deposits). Standard histopathologic parameters were analyzed by light, immunofluorescence and electron microscopy, with emphasis on glomerular and tubular basement membrane deposits, including Ig and PLA2R staining. Clinical data was reviewed in correlation with emphasis on primary hematological malignancy, HSCT parameters, time interval, course of GVHD, treatment and outcome.

Results: Eight biopsies/7 patients (6 males/1 female, age 48-70 years) were identified with membranous nephropathy and tubular basement membrane deposits. Clinically, 5 patients were transplanted for myeloproliferative disease (CML, CMML, AML), and 2 for multiple myeloma. Patients developed proteinuria after allogenic transplants (3-9.9 mg/mg, with hypoalbuminemia, at 15-61 months after HSCT). Six patients had active GVHD involving other organ systems at the time of biopsy (skin, GI, and/or lung). All patients had granular IgG and light chain staining along glomerular and tubular basement membranes. C3 was generally stronger in the tubules as compared to glomeruli. PLA2R was equivocal/weak in 2 and negative in the remainder. Six patients were treated with immunosuppression, including 4 with rituximab. One patient relapsed with biopsy proven persistence of the tubular basement membrane deposits.

Conclusions: We present a series of 7 HSCT patients with membranous nephropathy and concomitant tubular basement membrane deposits. This combination is seen in lupus or autoimmune disorders, and is otherwise rare. We hypothesize pathophysiology related to HSCT associated immune dysregulation or renal effects of GVHD underlie this injury. Further characterization of the target antigen (s) is needed to better understand the basis for this injury.

830 A Case of Mitochondrially Inherited Tubulointerstitial Kidney Disease

Alessia Buglioni[1], Linda Hasadsri[1], Samih Nasr[1], Marie Hogan[1], Ann Moyer[1], Khurrum Siddique[2], Mariam Priya Alexander[1]
[1]Mayo Clinic, Rochester, MN, [2]Doctors Hospital at Renaissance, Edinburg, TX

Disclosures: Alessia Buglioni: None; Samih Nasr: None; Khurrum Siddique: None; Mariam Priya Alexander: None

Background: Mitochondrial dysfunction has been previously described in cases of chronic kidney disease (CKD), and subjects affected by primary systemic mitochondrial disease may develop CKD. Examples of mitochondrially inherited tubulointerstitial kidney disease in subjects with no other symptomatic organ involvement have been recently reported.

Design: This is a case report of a 12-year-old boy who presented with short stature and work up showed bilateral hypoplastic kidneys (< 5th percentile), CKD stage 4 (GFR 27 ml/min/1.73m^2 BSA) along with comorbidities: anemia and secondary hyperparathyroidism. His mother and maternal uncle were on dialysis since their 30's due to end-stage renal disease of unknown etiology, and a 10-year-old half-brother (same mother) was managed for "Bartter syndrome".

Results: A diagnostic kidney biopsy was performed. Light microscopy showed mild chronic tubulointerstitial nephropathy. Immunofluorescence was negative. Electron microscopy showed markedly enlarged and dysmorphic mitochondria. Given this striking histopathologic finding, genetic testing was performed. Next generation sequencing of mitochondrial DNA from the biopsy showed the presence of a homoplasmic single missense mutation in position 616 (m.616T>C) of the mitochondrially encoded transfer RNA phenylalanine (*MTTF*) gene. After this unusual finding, we were able to analyze blood-derived mtDNA from mother and maternal uncle, and confirmed the same homoplasmic mitochondrial mutation. Further, we obtained a kidney biopsy from his half-brother, and also found the same pathologic features and mitochondrial mutation. The cytopathy was more prominent in the distal tubules, explaining the etiology of electrolyte losses and a Bartter-like phenotype. The renal biopsy findings, genetic findings, and pattern of inheritance are consistent with a diagnosis of mitochondrially inherited tubulointerstitial kidney disease in the family. No additional symptomatic organ involvement was present in these subjects.

Conclusions: Our case supports and reinforces the possibility of a kidney-limited mitochondrial disease, potentially radically changing management and prognosis of this family. Careful analysis of mitochondria by electron microscopy should be performed in patients with tubulointerstitial nephropathy and family history of kidney failure.

831 Punctate Visceral Epithelial IgG Immunoreactivity Associated with Podocytopathies Exhibits Heterogeneous Oligoclonality and Absence of Complement

Junbo Chen[1], Gabriel Lerner[2], Hui Chen[1], Astrid Weins[3], Joel Henderson[1]
[1]Boston Medical Center, Boston, MA, [2]Yale School of Medicine, Yale New Haven Hospital, New Haven, CT, [3]Brigham and Women's Hospital, Boston, MA

Disclosures: Junbo Chen: None; Gabriel Lerner: None; Hui Chen: None; Astrid Weins: None; Joel Henderson: *Grant or Research Support*, Pfizer

Background: Minimal changes disease (MCD) and related primary podocytopathies (Px) have traditionally been considered to lack immunoglobulin heavy chain (Ig), light chain or complement deposition. We have observed punctate IgG immunoreactivity (P-IgG) on routine immunofluorescence (IF) in many Px cases, including Minimal Change Disease (MCD), Primary Focal Segmental Glomerulosclerosis (pFSGS), and Lupus Podocytopathies (LPs). This delicate immunoreactivity does not co-localize with albumin protein reabsorption, and may represent disease specific autoimmunoreactivity against podocyte proteins (REFERENCE). Based on the observation of varying patterns of P-IgG clonality in routine practice, we sought to characterize the range of involved immunoglobulin subclasses associated with this phenomenon.

Design: We reviewed a series of archived renal biopsies from two institutions with a diagnosis of MCD, pFSGS, or LP, and +P-IgG on podocytes. A routine IF staining panel was performed for polyclonal IgG, kappa and lambda light chains, IgG subclasses IgG_1, IgG_2, IgG_3 and IgG_4, and complements C4d, C3, and C1q. Intensity of punctate immunoreactivity on podocyte cell bodies was graded on a 0 (no) to 4+ (severe) scale.

Results: The result of IF quantification of punctate podocyte staining for the case series is shown in **Table 1** (TL: tip lesion variant; NOS: Not otherwise specified; Tx: transplant biopsy). We found that the P-IgG exhibited reactivity characteristic of intact oligoclonal immunoglobulin, composed of one or more IgG heavy chain subclasses as well as one or both immunoglobulin light chain subclasses, as required for antigen recognition and binding. With the exception of one transplant biopsy, in no case did we observe significant complement staining. Representative epifluorescence micrographs of human kidney biopsies from 4 patients with minimal change disease (A-D) are seen in **Figure 1**, showing P-IgG with various combinations of heavy and light chain subclasses. Staining intensity is indicated parenthetically in each image; TR: trace; Scale bar = 10 mm.

ID No.	IgG	IgG1	IgG2	IgG3	IgG4	kappa	lambda	C4d	C3	C1q
MCD-1	3+	2+ - 3+	0	T,D	0	T,D	0	0	0	0
MCD-2	3+	2+	0	0	1+,D	0	3+	0	0	0
MCD-3	T	T,S	0	T	0	0	T,S	0	0	0
MCD-4	2+	T,DS	0	2+,S	2+	1+,D	T	0	0	0
MCD-5	3+	2+,D	0	0	1+,D	2+	T,D	0	0	0
MCD-6	2+	T	0	1+	2+	T	2+	0	0	0
MCD-7	2+	*	*	*	*	2+,S	1+ - 2+,S	0	0	0
MCD-8	1+	T	0	T - 1+	1+	T - 1+	T	0	0	0
MCD-9 (Tx)	4+	3+	0	2+ - 3+	0	3+ - 4+	2+	3+	0	0
MCD-10	T	0	0	0	T	0	T	0	0	0
MCD-11	2+	2+	0	T	1+	2+	T	0	0	0
MCD-12	3+	1+	0	2+ - 3+	2+	2+	1+	0	0	0
MCD-13	1+	T	0	0	0	T	0	0	0	0
MCD-14	2+	T - 1+	0	0	2+	T	1+ - 2+	0	0	0
MCD-15	3+	T	0	0	2+ - 3+	2+ - 3+	0	0	0	0
FSGS-1(NOS)	0	0	0	0	0	0	0	0	0	0
FSGS-2(NOS)	0	0	0	0	0	0	0	0	0	0
FSGS-3(TL)	0	0	0	0	0	0	0	0	0	0
FSGS-4(NOS)	0	0	0	0	0	0	0	0	0	0
FSGS-5(TL)	2+	2+	0	0	0	2+	1+ - 2+	0	0	0
FSGS-6(NOS)	0	0	0	0	0	0	0	0	0	0
FSGS-7(NOS)	3+	3+	1+	2+	T	0	3+	T	0	0
LP-1	2+	2+	0	0	0	1+	T	T	0	0

Figure 1 - 831

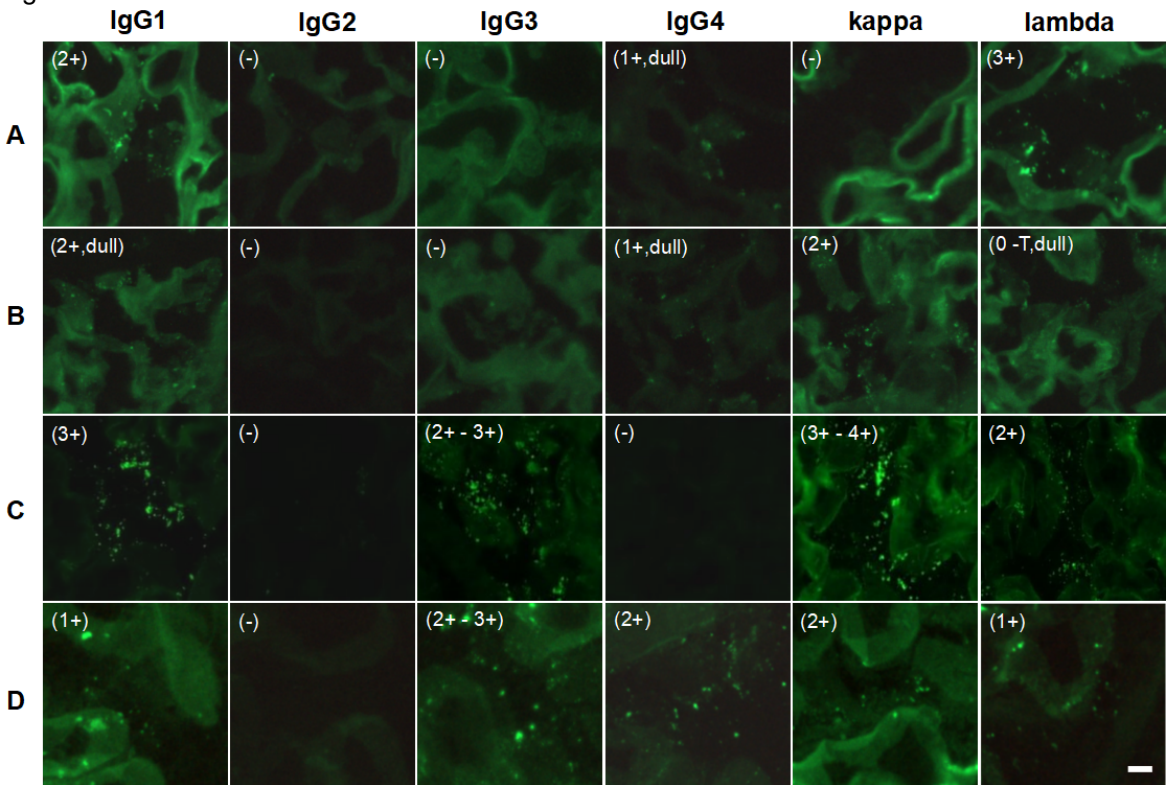

Conclusions: Our results suggest an antigen-autoantibody interaction occurring in MCD and related Px, albeit in the absence of outright immune complex deposition as evidenced by the lack of complement staining in P-IgG. Ultimately, these studies may help to reveal new mechanisms of direct podocyte injury in MCD and other related Px, and contribute to our understanding of podocyte pathophysiology.

832 A Contemporary Study of Pathologic Kidney Findings in Congenital Heart Disease

Bernadette DeRussy[1], Paul Miller[2], Neeraja Kambham[3], David Kwiatkowski[2], Darren Salmi[2], Megan Troxell[2]

[1]Stanford Pathology, Stanford, CA, [2]Stanford University Medical Center, Stanford, CA, [3]Stanford University, Stanford, CA

Disclosures: Bernadette DeRussy: None; Paul Miller: None; Neeraja Kambham: None; Darren Salmi: None; Megan Troxell: None

Background: Chronic kidney disease (CKD) is associated with both cyanotic and non-cyanotic congenital heart disease (CHD) and often develops during childhood. Several pathologic kidney findings in patients with CHD have been described; however, studies spanning early childhood to young adulthood in the modern era of cardiac surgery and transplantation are lacking and etiology of these findings is poorly understood.

Design: We searched the autopsy records of our academic center from January 2004 to May 2020 for patients with CHD for which at least gross examination of the heart and histologic examination of kidneys were performed. Chart review was performed to document related clinical parameters. Histologic sections of the kidneys were reviewed and scored for relevant pathologic parameters (glomerular size and morphology, intersitial fibrosis and tubular atrophy (IFTA), juxtaglomerular apparatus (JGA) hyperplasia, vascular changes, casts, other).

Results: Twenty-eight autopsy patients between the ages of 5 and 25 years were identified with CHD being the primary contributor to death. Twenty-six patients had undergone significant cardiac surgery, including 13 patients who had heart transplants. Average baseline serum creatinine was 0.7 mg/dL, 13 patients had hematuria, and 15

patients had proteinuria. On light microscopy, 10 patients had glomerulomegaly (>200 nm). Twenty patients had JGA hyperplasia, including 6 patients who did not undergo heart transplant (no calcineurin exposure). Four patients had focal segmental glomerulosclerosis (FSGS, predominantly perihilar variant), all of whom had glomerulomegaly. Nineteen patients had mesangial hypercellularity/expansion (>3 mesangial cells). Five patients had significant (>10%) IFTA. Megakaryocytes were identified in the glomeruli of 10 patients.

Figure 1. Histologic example of glomerulomegaly and FSGS

Figure 2. A normal size glomerulus with mild JGA hyperplasia, at same magnification

Table 1. Histopathology by glomerular size

Histopathology	Glomerular diameter <=200 nm	Glomerular diameter >200nm
FSGS*	0/18 (0%)	4/10 (40%)
IFTA >10%*	1/18 (6%)	4/10 (40%)
JGA hyperplasia	13/18 (72%)	7/10 (70%)
Mesangial hyperplasia/expansion	12/18 (67%)	7/10 (70%)
Megakaryocytes	6/18 (33%)	4/10 (40%)
Proteinuria	9/13 (69%)	6/6 (100%)
Hematuria	7/13 (54%)	6/6 (100%)
Average age (years)	11	16

*p<.05 by Fisher exact test

Figure 1 - 832

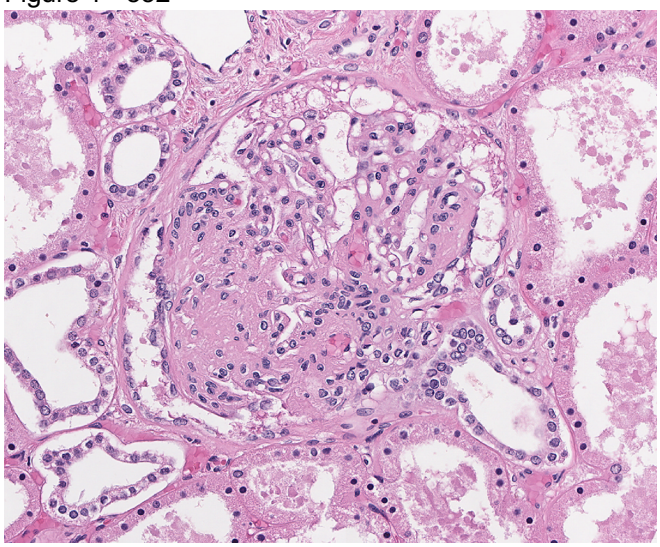

Figure 2 - 832

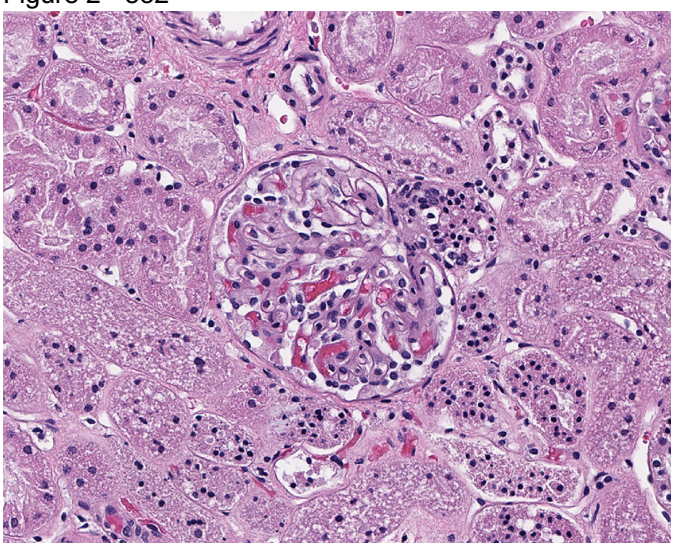

Conclusions: The pathophysiology of CHD is complex and dysregulated hemodynamic factors may be associated with kidney injury. At autopsy, our contemporary pediatric and young adult CHD cohort showed various clinical and pathologic findings (proteinuria, glomerulomegaly, JGA hyperplasia, and perihilar variant FSGS) that have been well-described in association with renal hyperfiltration injury and secondary FSGS. These features suggest that CHD may represent a significant risk factor for secondary FSGS and the pathogenesis may be similar to that seen in obese patients or those with low nephron endowment.

833 Clinicopathologic Features of a Cohort of Latin-American Patients with Monoclonal Immunoglobulin–Associated Renal Diseases

Lina Maria Espinosa Saltaren[1], Adriana Florez[2], Johanna Alvarez Figueroa[1], Rafael Andrade[1]
[1]Hospital Universitario Fundación Santa Fe de Bogotá, Bogota, Colombia, [2]Fundacion Santa Fe de Bogota, Bogotá, Colombia

Disclosures: Lina Maria Espinosa Saltaren: None; Rafael Andrade: None

Background: Monoclonal immunoglobulin–associated renal diseases encompass a group of diverse entities related to an underlying clonal proliferation of plasma cells or B lymphocytes. The majority of monoclonal immunoglobulin associated renal diseases results from direct deposition of the monoclonal immunoglobulin, either its light chain or heavy chain fragment, in the different renal compartments. They include light chain and/or heavy chain amyloidosis (AL/AH), monoclonal immunoglobulin deposition disease (MIDD), light chain proximal tubulopathy, light chain ("myeloma") cast nephropathy (MCN), proliferative glomerulonephritis with monoclonal immunoglobulin deposits, and type 1 cryoglobulinemia. This study aims to characterize these entities in a cohort of Latin-American patients with biopsy-proven monoclonal immunoglobulin-associated renal disease, diagnosed in a reference center for renal pathology in Colombia.

Design: The department database was searched for diagnosis of MCN, AL/AH, MIDD, light chain proximal tubulopathy, and immune complex type glomerulonephritis with monoclonal deposits, from January 2016 to December 2019. Clinicopathology features were recollected from the pathology reports and medical records when available.

Results: A total of 103 cases were retrieved. Overall, the male to female ratio was 1,5:1. Of the patients with a diagnosis of MCN, the pathogenic light chain most commonly detected was lambda, with a κ/λ ratio of 1:2. The majority of cases of amyloidosis were of the AL type, with the pathogenic light chain being more often lambda, with a κ/λ ratio of 1:14. Regarding MIDD, the majority of cases were of the light chain deposition disease type, more frequently with monotypic kappa light chain, with a κ/λ ratio of 3:1. All of the cases of light chain proximal tubulopathy corresponded to the “without crystals" type, and the most prevalent pathogenic light chain was lambda, with a κ/λ ratio of 1:8.

Of the 103 patients, 29 had a diagnosis of multiple myeloma, of which 22 were diagnosed with MCN, 5 with AH/AL, 4 with MIDD (3 with concomitant MCN), and 3 with tubulopathy (2 with concomitant MCN). This study is limited by its retrospective nature and shortage of clinical data from some referral centers.

	All patients	**MCN**	**Amyloid**	**MIDD**	**Proximal tubulopathy**	**IC mediated GN**
Nº of patients	103	42	36	19	9	9
Age						
Range	35 - 85	35 - 85	44 – 78	37 - 79	48 - 83	46 - 84
Mean (+/- SD)	60,9 (+/- 11)	61,8 (+/- 11,5)	60,0 (+/- 10,4)	58,5 (+/- 11,4)	62,4 (+/- 10,4)	64,6 (+/- 11,2)
< 50 y *n* (%)	22 (21%)	7 (17%)	10 (28%)	5 (26%)	1 (11%)	1 (11%)
51 – 70 y *n* (%)	62 (60%)	27 (64%)	20 (55%)	11 (58%)	6 (67%)	5 (56%)
> 70 y *n* (%)	19 (19%)	8 (19%)	6 (17%)	3 (16%)	2 (22%)	3 (33%)
Sex						
Male *n* (%)	61 (59%)	26 (62%)	18 (50%)	12 (63%)	5 (56%)	5 (56%)
Female	42 (41%)	16 (38%)	18 (50%)	7 (37%)	4 (44%)	4 (44%)

n (%)						
Type						
LC only *n* (%)			29 (80%)	16 (84%)		8 (89%)
Kappa *n* (%)		15 (36%)	2 (7%)	12 (75%)	1 (11%)	2 (25%)
Lambda *n* (%)		27 (64%)	27 (93%)	4 (25%)	8 (89%)	6 (75%)
LC + HC *n* (%)			6 (17%)	2 (11%)		1 (11%)
HC only *n* (%)			1 (3%)	1 (5%)		
Laboratory						
Mean sCr (+/- SD) mg/dL		6,7 (+/- 4)	1,6 (+/- 0,8)	4,8 (+/- 3,2)		
Proteinuria present *n*		13	29	8	6	5
Nephrotic range proteinuria or Nephrotic syndrome present *n* (% of patients with proteinuria)		7 (54%)	21 (72%)	4 (50%)	2 (33%)	3 (60%)
SD = Standard Deviation, LC= Light Chain, HC=Heavy Chain, sCr=Serum creatinine						

Conclusions: Compared to other cohorts, MCN in our cohort showed lambda predilection, in contrast to the usual kappa predominance. A diagnosis of monoclonal immunoglobulin–associated renal diseases should not be disregarded in the younger population since 21% of patients were younger than 50 years old. In our cohort, certain clinical features favored a diagnosis, for example, a diagnosis of amyloidosis was most likely when nephrotic range proteinuria or nephrotic syndrome was present, as well as a higher possibility of MCD in the presence of very high serum creatinine. However, these clinical features are not specific, and a renal biopsy is always required to confirm a clinical suspicion.

834 Duration and Magnitude of BK Viremia Do Not Predict Outcome in Patients After Kidney Transplantation

Evan Farkash[1], Mona Doshi[1]
[1]*University of Michigan, Ann Arbor, MI*

Disclosures: Evan Farkash: None; Mona Doshi: None

Background: BK polyomavirus nephropathy was a major cause of kidney transplant failure in the early 2000's and remains a risk factor for subsequent rejection. The standard of care at our large transplant center now includes frequent testing for BK viremia and early reduction in immunosuppression. What are the features and outcomes of BK infection in the setting of aggressive monitoring and treatment?

Design: We retrospectively analyzed the demographics and outcomes of 401 renal transplant recipients with BK viremia from 2/2006 to 8/2017. Demographic data, transplant type and outcome, biopsy reports, and BK viremia tests were collected from electronic medical records and laboratory information systems. Demographic data was

analyzed by chi-squared and Fisher exact tests, and survival data was analyzed by effect likelihood ratio. (JMP v15, SAS).

Results: During the study period, there were roughly 2550 kidney transplants, corresponding to a 15.6% rate of BK viremia. Patients with BK viremia were of similar gender (253/401, 63.1% male) compared to the overall transplant population (62.2% male; p=0.74 by Fisher exact). 127 patients (31.7%) with BK viremia were non-white (97 African-American, 10 Asian, 20 Native American and other), similar to regional demographics. The proportion of living related (15.2%), living unrelated (23.9%), and deceased donor (60.8%) transplants were also similar to the overall transplant population (17.8%, 23.6%, and 58.6%; p=0.43 by chi-squared). In patients with BK viremia, there was no association between peak BK titer and risk of graft failure (p=0.93, likelihood ratio) or combined failure/death (p=0.98). Duration of BK infection correlated with better outcome (p=0.019 and 0.032), likely due to length bias. Graft half-life was similar for patients with BK viremia and nationally reported graft survival (deceased ~13 years, living ~16 years).

Conclusions: Kidney transplant recipients with BK viremia are demographically similar to the overall transplant population. In comparison to historical reports, BK infection does not affect graft failure and overall survival in a modern, aggressively managed cohort. Within the cohort of patients with BK viremia, severe or persistent infections also do not predispose to poor outcome. There were 734 biopsies on 348 of the patients in the study during active BK viremia or within 6 months after viral clearance, and future studies will examine the influence of histologic features during and after infection on graft survival.

835 The Prevalence of Mesangial Electron Dense Deposits in PLA2R-Positive Membranous Nephropathy

Gabriel Giannini[1], Lois Arend[1]
[1]*Johns Hopkins School of Medicine, Baltimore, MD*

Disclosures: Gabriel Giannini: None; Lois Arend: None

Background: Membranous nephropathy (MN) is a common cause of nephrotic syndrome in adults and is caused by formation of antigen-antibody immune complexes in the subepithelial region of the glomerular basement membrane. The antigenic target of antibodies in 70% of cases is PLA2R. The presence or absence of mesangial electron dense deposits has been used to help delineate between primary MN and secondary MN. Mesangial deposits in primary MN were initially described to occur in approximately 10% of cases, and their presence is thought to suggest MN due to lupus, infections, or other causes. An immunohistochemical (IHC) stain for PLA2R is now routinely used for confirming a diagnosis of primary MN. If mesangial deposits predict a secondary cause they should be more frequent in PLA2R-negative patients.

Design: A review of all institutional cases between 3/2017 and 6/2020 identified all cases of MN. These biopsy specimens were received for diagnosis and interpretation between March of 2017 and July 31 2020. Cases with a diagnosis of lupus or near “full house” staining by immunofluorescence microscopy (IF) were excluded. Light microscopy, IF, and electron microscopy (EM) were performed in each case of MN. PLA2R positivity was determined by either IF or IHC. Five cases did not have PLA2R staining, and were excluded. EM for all cases was reviewed, blinded to PLA2R status, and electron dense deposit locations and stage were recorded. Membranous reaction was staged using the Ehrenreich and Churg system.

Results: 94 cases of membranous nephritis with PLA2R staining were identified. The mean age was 56.18, ranging from 15 to91-years-old. The male:female ratio was 1.3 (40 female, 52 male). 48 patients had stated ethnicities and included: 4 asian, 20 black, 5 hispanic, 16 white, and 3 other. 52 cases (58%) were positive and 35 were negative for PLA2R. 23 (25%) had mesangial electron dense deposits; including 11 PLA2R positive and 12 PLA2R negative cases. 28.8% (11/52) of PLA2R-positive cases had mesangial deposits, while 34.3% (12/35) of negative cases had mesangial deposits.

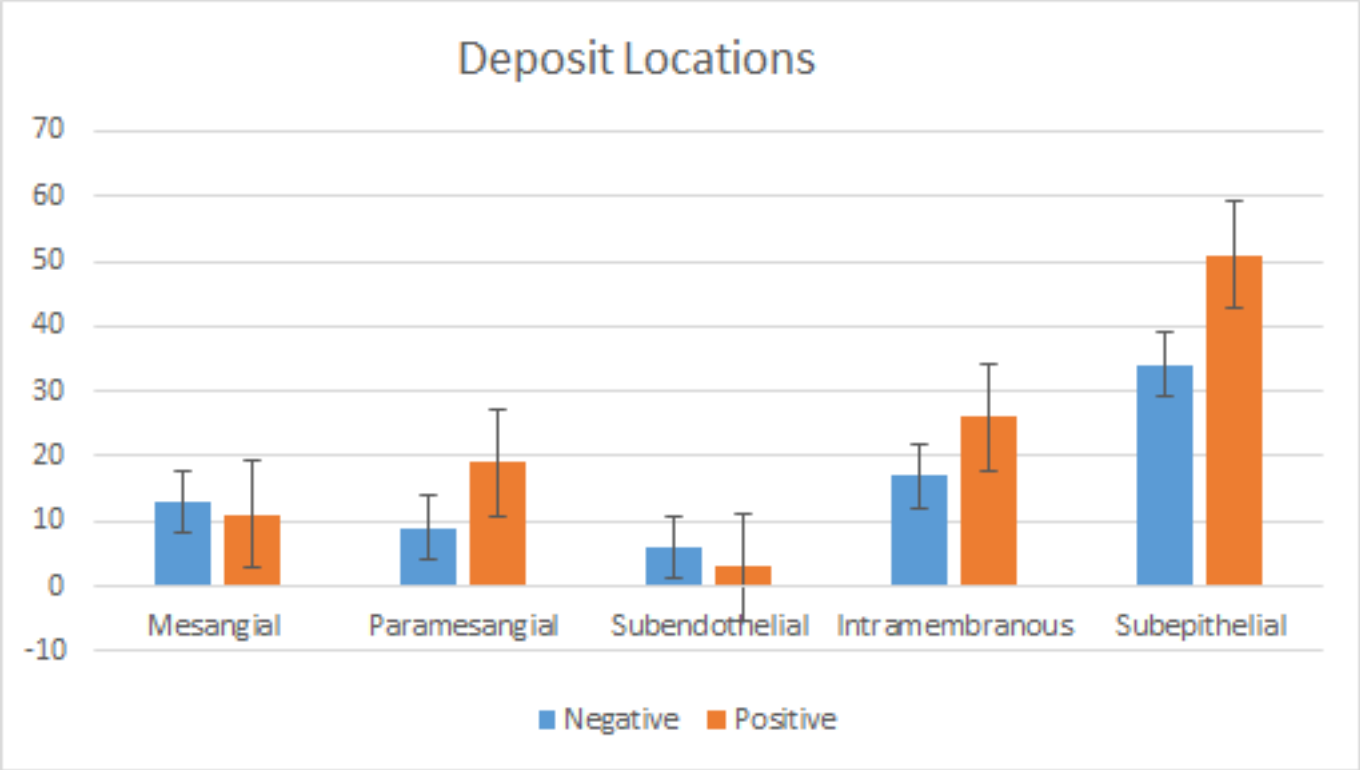

Conclusions: PLA2R negative cases were only 1.2 times more likely to have mesangial deposits. PLA2R positivity did not change the frequency of mesangial electron dense deposits in MN. The increased frequency (10-25%) of mesangial deposits in primary MN found in this study may be due to population sampling differences or under-reporting of mesangial deposits in historical studies.

836 Long-Standing Donor Diabetes, Recipient Diabetes, and Pathologic Findings are Associated with Shorter Kidney Allograft Survival in Patients who Receive Kidney Transplants from Diabetic Donors

Aubre Gilbert[1], David Scott[1], Megan Stack[1], David Woodland[1], Angelo de Mattos[1], Shehzad Rehman[1], Joe Lockridge[1], Douglas Norman[1], Vanderlene Kung[1], Nicole Andeen[1]
[1]Oregon Health & Science University, Portland, OR

Disclosures: David Scott: None; Angelo de Mattos: None; Nicole Andeen: None

Background: Approximately 6% of deceased kidney donors (DKD) are diabetic; these kidneys may be associated with worse allograft survival, but recipient diabetes status has a greater impact on graft mortality and survival. Since biopsy findings are a common reason for organ discard, we sought to understand the histologic and clinical factors that influence graft survival in patients who receive a kidney from a diabetic DKD.

Design: We retrospectively reviewed our institutional experience with diabetic DKD from 2005-2019, and re-evaluated pre-implantation and earliest post-transplant biopsies (usually at 3 months). Histologic findings were compared against a control cohort of non-diabetic DKD (n=107). Statistics were performed in GraphPad Prism 8 and Stata.

Results: 34 patients received kidney transplant from diabetic DKD, 25 of whom had biopsy information available (56 biopsies). Compared against a control cohort of non-diabetic DKD, kidneys from diabetic DKD had significantly greater non-glomerular chronic injury (Figure). Arteriosclerosis (88%) and arteriolar hyalinosis (54%) were the most common lesions in allograft kidney biopsies from diabetic DKD. Classic diabetic glomerulopathy was less prevalent, seen in 29% of biopsies and usually manifest as mild or diffuse mesangial sclerosis (21%), with only 8% (2 recipients from same donor) showing nodular glomerulosclerosis.

Five patients experienced graft failure in our study period. There was no difference in death-censored graft survival for either all-comers or diabetic recipients who received transplants from a diabetic DKD versus non-diabetic DKD. However, donor diabetes greater than 10 years was associated with graft failure (HR 11.5, p=0.04). Diabetic recipients had shorter graft survival, regardless of donor diabetes status. Of histologic variables seen on 3 month biopsy, diabetic glomerulopathy (p=0.01), moderate tubular atrophy and interstitial fibrosis (IFTA, p=0.02), and moderate arteriolar hyalinosis (p=0.01) were associated with allograft failure. On pre-implantation frozen sections from diabetic DKD, arteriolar hyalinosis (p=0.03) and IFTA (p=0.03) were associated with graft failure, but arteriosclerosis and global glomerulosclerosis scores were not.

Figure 1 - 836

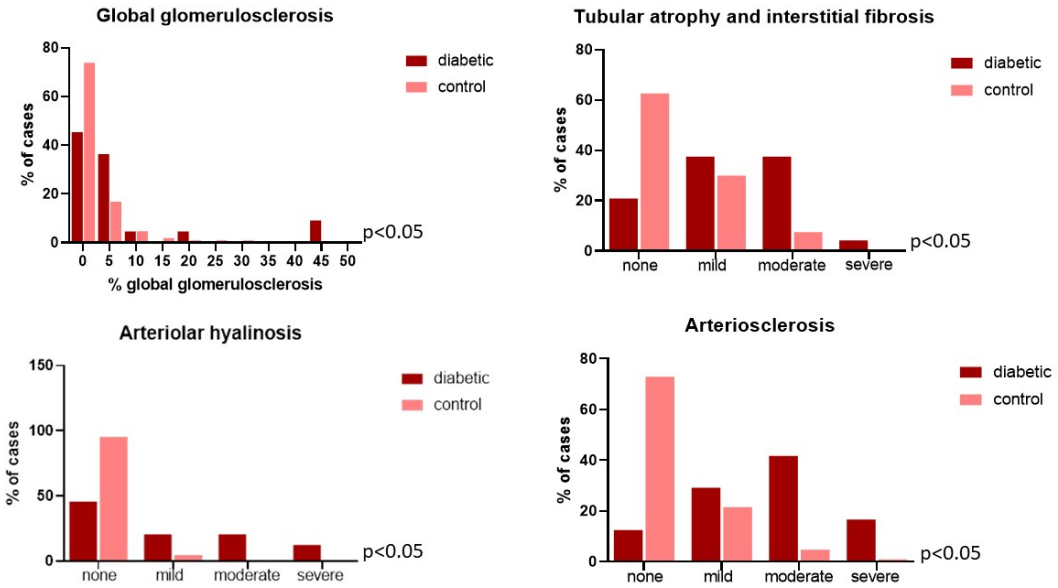

Conclusions: Donor diabetes greater than 10 years, recipient diabetes, and histologic findings on early post-transplant biopsy negatively impact graft survival in patients with who receive kidney transplants from diabetic donors.

837 First In-vivo Evidence of Renal Phospholipidosis Induced by Amlodipine

Karam Han[1], Santhi Ganesan[1], Hope Hastings[2], Agnes Loeffler[3]
[1]MetroHealth Medical Center, Cleveland, OH, [2]Oklahoma University Health Sciences Center, Oklahoma City, OK, [3]MetroHealth System, Case Western Reserve University, Cleveland, OH

Disclosures: Karam Han: None; Santhi Ganesan: None; Hope Hastings: None

Background: Fabry Disease (FD), a lysosomal storage disorder caused by alphagalactosidease A deficiency, is known to produce electron-dense lipid-like deposits or "zebra bodies" on electron microscopy. Similar ultrastructural deposits are also seen in patients on certain drugs, such as hydroxychloroquine and aminoglycosides. There has been an vitro study that demonstrated an increase in phospholipid levels by other potential drugs with similar cationic amphiphilic properties using silico model, but little clinical data exists concerning these additional cationic amphiphilic substances to support the hypothesis and their phospholipidosis-inducing potential in patient specimen.

Design: We identified two cases of phospholipidosis from the renal biopsy of the patients who are on potential cationic amphiphilic drugs described in the in-vitro studies. We reviewed existing literature and designed a case control study based on the patients' relevant clinical history to assess whether the renal phospholipidosis seen on ultrastructural examination are caused by potential drug effects or different comorbidities, i.e. plasma cell

dyscrasias. Autopsy and surgical cases with plasma cell dyscrasia (n=10) were included as controls. The cases without the previous electron microscopy (EM) were submitted and reviewed for possible drug-induced lysosomal phospholipidosis.

Results: Presence of lysosomal phospholipidosis by electron microscopy was confirmed on two cases , one with amlodipine and another with carvedilol, both of which were previously described in experimental, in vitro model but not in clinical setting. However, the second case was deemed less likely due to carvedilol because of the short duration. Both cases revealed unique osmiophilic inclusions within glomerular podocytes while the background kidney showed tubulo-interstitial changes keeping with early cast nephropathy and tubular injury or early tubular necrosis. No features of acute/allergic interstitial nephritis were present. Among our control cases, one patient with history of elevated kappa light chain showed amyloidosis by electron microscopy, but without intracytoplasmic, lamellar structures.

Figure 1 - 837

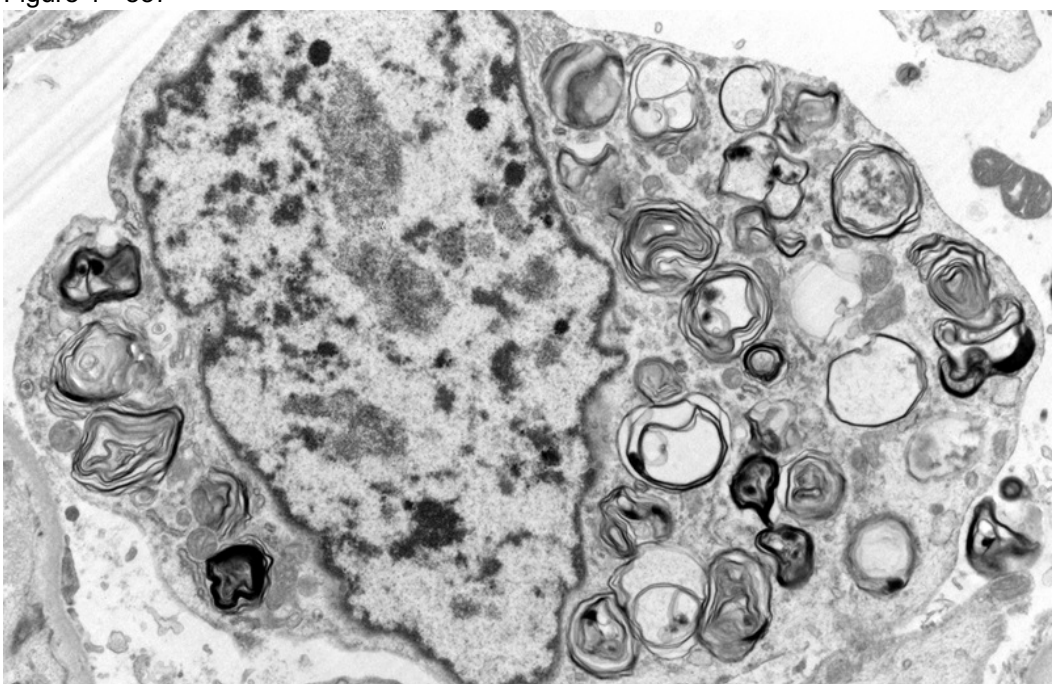

Conclusions: In this study, we identified in vivo evidence of new potential renal phospholipidosis inducing agents including amlodipine, a calcium channel blocking agent used for anti hypertensive treatment. Future studies are needed to establish potential drug-induced phospholipid inclusion as renal effects of these drugs.

838 Definitive Characterization of Protein Reabsorption Granules vs. Punctate IgG Immunoreactivity in Primary Podocytopathies

Tochukwu Ihejirika[1], Junbo Chen[2], Morgan Thompson[1], Gabriel Lerner[3], Laurence Beck[4], Ivy Rosales[5], Andrew Watts[6], Keith Keller[7], Hui Chen[2], Astrid Weins[7], Joel Henderson[2]
[1]Boston University School of Medicine/Boston Medical Center, Boston, MA, [2]Boston Medical Center, Boston, MA, [3]Yale School of Medicine, Yale New Haven Hospital, New Haven, CT, [4]Boston University School of Medicine, Boston, MA, [5]Massachusetts General Hospital, Boston, MA, [6]Brigham and Women's Hospital, Harvard Medical School, MA, [7]Brigham and Women's Hospital, Boston, MA

Disclosures: Tochukwu Ihejirika: None; Junbo Chen: None; Morgan Thompson: None; Gabriel Lerner: None; Laurence Beck: None; Andrew Watts: None; Keith Keller: None; Hui Chen: None; Astrid Weins: None; Joel Henderson: *Grant or Research Support*, Pfizer

Background: Current diagnosis of primary podocytopathies (Px), such as Minimal Change Disease (MCD), Primary Focal Segmental Glomerulosclerosis (FSGS, pFSGS), and Lupus Podocytopathies (LPs), currently relies on technically-exhaustive electron microscopy analysis to determine both disease entity and severity. We and others have observed punctate IgG immunoreactivity (P-IgG) on routine immunofluorescence in many Px cases, that may represent disease-specific autoimmunoreactivity. However, P-IgG may be interpreted as epithelial protein reabsorption and its significance as a potential marker for Px may be missed. We sought to characterize key features of protein reabsorption granules (PRGs) and P-IgG, which may help to differentiate these features and facilitate the rapid diagnosis of Px through immunofluorescence microscopy (IF).

Design: We investigate these two morphologic features in a study of archival material.

We conducted IF on archived biopsies from cases of Px and control cases including secondary FSGS (sFSGS). Anti-human IgG and anti-human albumin staining was evaluated by assessing key morphologic characteristics such as location, distribution, and size of stained punctate features.

Results: The P-IgG pattern was seen in almost all MCD cases but was absent in the sFSGS. Protein reabsorption granules were present across case types in glomerular and tubular epithelial cells, in the absence or presence of the P-IgG. The albumin PRGs were usually coarse and clustered, and were observed focally and segmentally in the glomeruli. In contrast, the P-IgG was finer (smaller in size), more uniform in size, and almost always diffuse and global in the glomeruli

Difference in Morphological Characteristics between P-IgG and PRGs		
Characteristic	**P-IgG**	**PRG**
Disease Type	Px	sFSGS; Px
Location	Podocyte	Tubules; Glomeruli
Distribution	Diffuse; Global	Focal; Segmental
Size	Fine	Coarse
Shape	Punctate	Clustered
Expected Protein Composition	IgG; kappa & lambda	Albumin in combination with various immunoreactants

Conclusions: The PRGs, as shown by anti-albumin staining, did not colocalize with P-IgG. P-IgG is distinct from PRGs in makeup, location, and size, indicating separate etiology. Therefore the P-IgG observed in Px is highly likely to represent a distinct process from epithelial protein reabsorption. Additional studies using antibodies for megalin and cubilin, specific markers for PRGs, are underway.

839 Squalene in Prevention of Podocyte Injury

Resmiye Irmak Yuzuguldu[1], Osman Yılmaz[2], Mehtat Unlu[2], Hatice Kolatan[1], Hulya Ellidokuz[2], Caner Cavdar[2], Hulya Guven[1], Sulen Sarioglu[3]
[1]Dokuz Eylul University School of Medicine, Izmir, Turkey, [2]Dokuz Eylul University School of Medicine, Balcova, Turkey, [3]Dokuz Eylul University School of Medicine, Balçova, Turkey

Disclosures: Resmiye Irmak Yuzuguldu: None; Osman Yılmaz: None; Mehtat Unlu: None; Hatice Kolatan: None; Hulya Ellidokuz: None; Caner Cavdar: None; Hulya Guven: None; Sulen Sarioglu: None

Background: Focal segmental glomerulosclerosis (FSGS) is a frequent renal disease related to podocyte injury. There is no treatment regimen that can provide remission in all FSGS patients, and the rate of recurrence can be up to 40%. Squalene is an isoprenoid compound found mainly is shark liver and olive oil. Studies related to squalene are focused on antioxidant and antitumoral effects. This study aims to investigate the effects of olive oil (SQ-O) and shark-derived squalene (SQ-S) on podocyte injury in an experimental animal model.

Design: Wistar rats with similar weights (300-350 g) were grouped as follows: control (n=7), SQ-S (n=7), SQ-O (n=6), Adriamycin (ADR) (n=7), SQ-S+ ADR (n=6) and SQ-O+ADR (n=7). Squalene was administered at a total dose of 0.4 ml/day for 14 days. One week after the SQ, intravenous ADR (7.5 mg/kg) was administered. Urine proteinuria, creatinine and urea values were analyzed in 24-hour urine on the 14th and 22rd days. Blood creatinine, blood urea nitrogen (BUN), total protein and albumin values were analyzed at the 23rd (sacrification day).

Hematoxylin & eosin, periodic acid schiff (PAS), trichrome, silver metanamine (PAMS) and Wilms' tumor 1 protein (WT-1) stained sections from the kidney tissues were evaluated by light microscopy (Figure-1). Bowman and glomerular tuft area were measured digitally. The mean segmental sclerosis scores were determined separately in PAS and PAMS stained sections (Figure-2). WT-1 positive podocytes were counted in 30 glomeruli. Tubular atrophy, interstitial fibrosis and inflammation, tubular damage was scored and thrombotic microangiopathy (TMA) findings were noted.

Results: All parameters were increased in ADR group compared to control, except for urine creatinine, urea; blood total protein, albümin and glomerular WT-1counts which were decreased as expected (p<0,05). There was no statistically significant difference between the SQ-O+ADR and the control group for most parameters; except for urine creatinine, urea and blood total protein, albumin values but all parameters were better than ADR group. Urine proteinuria and BUN in SQ-S+ADR were increased compared to ADR group, all other parameters were better than ADR group. Urine creatinine, urea, protein and blood BUN, total protein, albumin values between groups SQ-S+ADR worse than control group, probably related to the TMA findings detected in 3 rats belonging to SQ-S+ADR group (Table-1).

Groups	Control	SQ-S	SQ-O	ADR	SQ-S+ADR	SQ-O+ADR
14.rd day **U_P (g/24h)**	0.029 ± 0.006	0.024 ± 0.01	0.028 ± 0.02	0.725 ± 0.11	0.877 ± 0.14	0.662 ± 0.09
22.th day U_P (g/24h)	0.024 ± 0.004	0.021 ± 0.006	0.025 ± 0.01	0.824 ± 0.26	-	0.32 ± 0.06
BUN (mg/ dl)	18.3 ± 1.94	17.1 ± 1.96	19.0 ± 4.31	34.9 ± 11.8	71.9 ± 53	35.4 ± 10.5
Blood creatinine (mg/dl)	0.26 ± 0.051	0.28 ± 0.03	0.26 ± 0.02	0.44 ± 0.06	0.32 ± 0.1	0.33 ± 0.03
Bowman area	15001 ±1507	16362 ±661	15683 ±1638	10316 ±1115	15433 ±2448	13395 ±1613
Glomerular tuft area	10540 ±1507	11427 ±348	10849 ±1134	6803 ± 1076	9109 ± 748	8516 ± 841
SSS - PAS	0.0017 ± 0.002	0.0021 ± 0.001	0.0038 ± 0.003	0.2957 ± 0.09	0.115 ± 0.78	0.1083 ± 0.26
SSS - PAMS	0.001 ± 0.001	0.001 ± 0.001	0.004 ± 0.002	0.282 ± 0.079	0.103 ± 0.095	0.101 ± 0.014
WT-1	11.51 ± 0.14	11.51 ± 0.14	14.71 ± 1.52	7.15 ± 0.64	9.99 ± 2.51	11.86 ± 1.50

Table-1: Mean Values of the Clinicopathological Parameters Evaluated in Wistar Rat Groups.

All data are presented as mean ± SD.

Abbreviations: SQ: Squalane; SQ-S: Shark derived SQ administered group; SQ-O: Olive oil derived SQ administered group; ADR: Adriamycin administered group; SQ-S+ADR: Shark derived SQ and Adriamycin administered group; SQ-O+ADR: Olive oil derived SQ and Adriamycin administered group, U_P, urinary protein; BUN: *Blood urea* nitrogen; SSS: segmental sclerosis score.

* There was no statistical differences between any of these three groups (p< 0.05).
** Since 3 of the rats belonging to this group died early, urine samples of the remaining rats could not be collected and were sacrificed early (20th day).
¥ There was no statistical differences between control vs. SQ-O+ADR (p< 0.05).
φ There was no statistical differences between control vs. SQ-O+ADR (p< 0.05).
Θ There was no statistical differences between control vs. SQ-S+ADR and control vs. SQ-O+ADR (p< 0.05).
ᵀ There was no statistical differences between control vs. SQ-S+ADR and control vs. SQ-O+ADR (p< 0.05).
ᵖ There was no statistical differences between control vs. SQ-S+ADR and control vs. SQ-O+ADR (p< 0.05).
¶ There was no statistical differences between control vs. SQ-S+ADR and control vs. SQ-O+ADR (p< 0.05).
§ There was no statistical differences between control vs. SQ-S+ADR and control vs. SQ-O+ADR (p< 0.05).
€ ADR vs. SQ-O+ADR, p=0.031.

Figure 1 - 839

Figure-1: Significant loss of podocytes in group receiving Adriamycin (B), compared to control group (A). Note the preservation of the podocytes in groups receiving Adriamycin + Shark derived squalene (C) and Adriamycin + Olive oil derived squalene (B).
(IHC, WT1 original magnification X40)

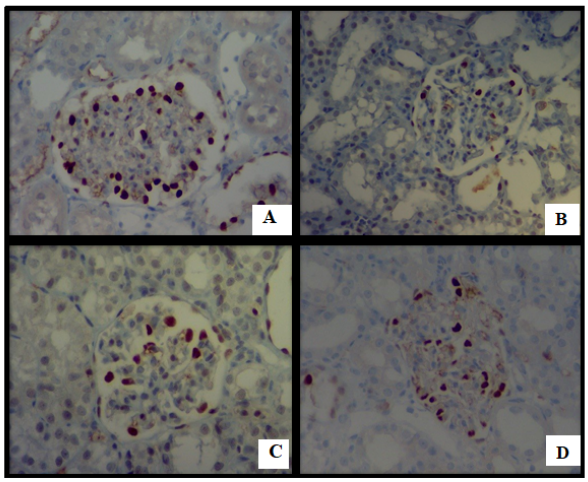

Figure 2 - 839

Figure-2: Glomeruli in control group (A), Adriamycin group (B) with severe segmental sclerosis affecting more than 75% of the tuft area. Less severe segmental sclerotic lesions in groups receiving Adriamycin + Shark derived squalene (C) and Adriamycin + Olive oil derived squalene (D).
(HC, PAMS original magnification X40)

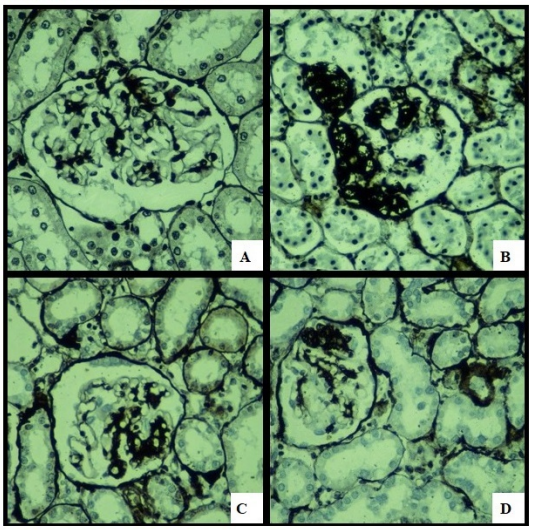

Conclusions: Olive oil derived squalene seems to be a valuable compound against podocyte injury which deserves further investigation to understand effector mechanisms and clinical availability.

840 Urinary Proteomics Data Guides AI to Discover New Digital Biomarkers for Diabetic Nephropathy Classification

Nicholas Lucarelli[1], Brandon Ginley[1], Seung Seok Han[2], Pinaki Sarder[1]
[1]SUNY Buffalo, Buffalo, NY, [2]Seoul National University College of Medicine, Seoul, South Korea

Disclosures: Nicholas Lucarelli: None; Brandon Ginley: None; Seung Seok Han: None; Pinaki Sarder: None

Background: Diabetic Nephropathy (DN) is one of the most common causes of end stage renal disease (ESRD). The Tervaert classification is a system for classifying the severity of DN using glomerular lesions. However, the resulting diagnoses do not perfectly predict patient progression. Significant literature suggests tubules are important to the pathogenesis of DN, but common assessment methods are limited to semi-quantitative estimation of IFTA. Further, urinary proteomics have proven to be a powerful tool to monitor disease progression. We used machine learning to study the structural changes in renal glomeruli, tubules, and urine of DN patients and their association with patient outcome.

Design: We studied whole slide images (WSIs) of periodic acid-Schiff stained renal biopsies from 56 DN patients matched with 2038 proteins measured from each patient's urine. Using Seurat, we identified proteins that were differentially expressed in patients that developed ESRD within 2 years after biopsy. Glomeruli, globally sclerotic glomeruli, tubules, arteries and arterioles, and interstitium were segmented from WSI using our previously published HAIL (human-AI-loop) for convolutional network training and prediction on WSIs. For each glomerulus, 315 handcrafted digital image features were measured, and for tubules, 207 features. Glomerular and tubular image features were used separately as inputs to a recurrent neural network to predict the patient's ESRD status within 2 years post-biopsy. Differentially expressed urine proteins were also used as inputs to a fully connected neural network to predict ESRD within 2 years.

Results: Urine proteins predicted DN progression to ESRD within 2 years with Cohen's Kappa, k = 0.91. Digital image features from renal glomeruli predicted progression with k = 0.14, while image features from renal tubules predicted progression with k = 0.49.

Conclusions: Our results suggest that urinary proteomics measurement almost perfectly predicted ESRD within 2 years. Our results also found features measured at the individual tubule level had higher prognostic power than the corresponding glomerular features. Thus, we believe both urine proteomics and computational biopsy histology should be leveraged in unison to develop an improved DN classification tool.

841 Unique Clinicopathologic Findings in Adenovirus Nephritis

Rebecca May[1], Tiffany Caza[1], Clarissa Cassol[1], Patrick Walker[1], Thomas Bourne[1], Nidia Messias[1], Zeljko Dvanajscak[1], Shree Sharma[1], L. Nicholas Cossey[1], Chris Larsen[1]
[1]Arkana Laboratories, Little Rock, AR

Disclosures: Rebecca May: None; Tiffany Caza: None; Clarissa Cassol: None; Thomas Bourne: None; Nidia Messias: None; L. Nicholas Cossey: None; Chris Larsen: None

Background: Adenovirus (AdV) infection is a severe complication within renal allografts that can mimic allograft rejection. The aim of this study is to describe the unique clinicopathologic findings of AdV nephritis through a retrospective analysis, by comparing the pathologic findings to cytomegalovirus (CMV) and polyomavirus (PV) nephritis.

Design: A blinded pathologic analysis was performed on AdV (n=8) and CMV (n=13) nephritis cases received at our institution from 1/1/2009-9/1/2020, and randomly selected PV nephritis cases (n=18) received from 1/1/2020-9/1/2020. Cases were distributed among renal pathologists who scored histologic findings. Clinical information was provided from the patient's nephrologist for clinicopathologic correlation.

Results: AdV nephritis displays frequent interstitial and tubular granulomas, and uniquely shows interstitial granulomas surrounding tubular granulomas (concentric granulomas). AdV nephritis shows increased inflammation and tubulitis compared to CMV and PV nephritis, but levels of interstitial fibrosis and tubular atrophy are similar. AdV nephritis shows predominantly histiocytic and plasma cell interstitial inflammation, whereas CMV nephritis shows predominantly lymphocytic and PV nephritis shows lymphocytic and plasma cell infiltrates. Necrosis and interstitial hemorrhage is more prevalent in AdV nephritis, as is Tamm-Horsfall extravasation. As expected, AdV inclusions are predominantly nuclear, CMV inclusions are nuclear and cytoplasmic, and PV inclusions are nuclear. (Table 1, Figure 1, Figure 2)

	AdV Nephritis	CMV Nephritis	PV Nephritis
N	8	13	18
Granulomas	6(75%)*	1(8%)	2(11%)
Tubular Granulomas	6(75%)*	0(0%)	1(6%)
Concentric Granulomas	6(75%)#	0(0%)	0(0%)
Necrosis	4(50%)*	0(0%)	1(6%)
Interstitial Hemorrhage	4(50%)*	0(0%)	3(17%)
TH Extravasation	5(63%)*	0(0%)	2(11%)
Interstitial Edema	8(100%)#	8(62%)	11(61%)
Acute Tubular Injury	8(100%)	13(100%)	18(100%)
Inflammation Score	2.75	1.69	2
Predominant Type of Inflammation	Histiocytes (5/63%) Plasma Cells (4/50%) Lymphocytes (3/38%)	Histiocytes (2/15%) Plasma Cells (1/8%) Lymphocytes (8/62%)	Histiocytes (1/6%) Plasma Cells (7/39%) Lymphocytes (11/61%)
Tubulitis Score	2.88	1.46	2.39
Interstitial Fibrosis Score	1.13	1.38	2
Tubular Atrophy Score	1.38	1.46	1.8
Viral Inclusions	5(63%)	5(38%)	9(50%)

Viral Inclusion Appearance	Nuclear (4/80%) Cytoplasmic (1/20%) Ground Glass (3/60%) Chromatin Margination (0/0%)	Nuclear (4/80%) Cytoplasmic (3/60%) Ground Glass (3/60%) Chromatin Margination (0/0%)	Nuclear (9/100%) Cytoplasmic (0/0%) Ground Glass (7/78%) Chromatin Margination (3/33%)

Table 1: Summary of Histologic Findings in AdV Nephritis, CMV Nephritis, and PV Nephritis. Average Banff Scoring was used for interstitial inflammation, tubulitis, interstitial fibrosis, and tubular atrophy. Predominant type of inflammation may be more than one type per case. AdV Nephritis was compared to the combined group of CMV Nephritis and PV Nephritis, and a $p<0.05$ is indicated by a (*) for the Mann-Whitney test and a (#) for the Wilcoxon test.

Figure 1 - 841

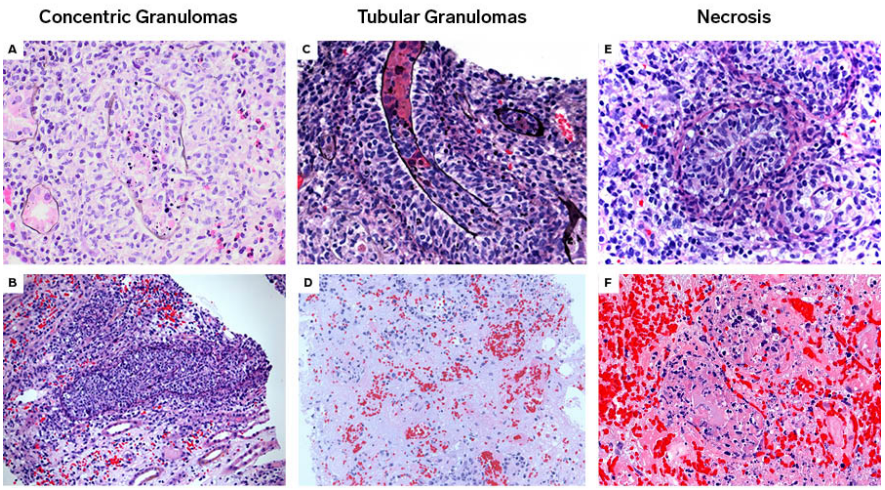

Figure 1: AdV Nephritis shows unique histopathologic features. A/B) Interstitial granulomas surrounding tubular granulomas (concentric granulomas), silver stain; C/D) Intratubular granulomas are most frequent in AdV Nephritis, silver stain; E/F) Necrosis is common in AdV Nephritis, H&E stain.

Figure 2 - 841

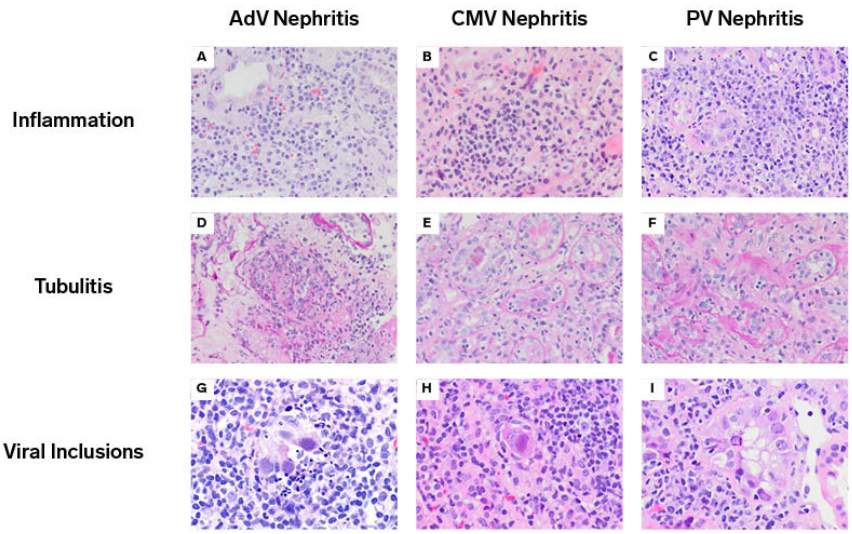

Figure 2: Inflammation, tubulitis, and viral inclusions in AdV Nephritis, CMV Nephritis, and PV Nephritis. A-C) Plasma cells and histocytes are predominant in AdV (A), lymphocytes in CMV (B), and lymphocytes and plasma cells in PV(C); D-F) Tubulitis is common in viral nephritis, with AdV showing tubular necrosis; G-I) Viral inclusions are largely nuclear in AdV (G) and PV (I), and nuclear and cytoplasmic in CMV (H).

Conclusions: AdV nephritis uniquely displays concentric granulomas, as well as more severe tubulitis and inflammation (histocytic and plasma cell dominant). Necrosis is prominent in AdV nephritis. These histologic findings should prompt immunohistochemical staining for AdV in tissue sections, especially when differentiating between allograft rejection and infection.

842 Nephropathology of Coronavirus 2019 Disease (COVID-19): A Multi-Center Retrospective Cohort Study by the COVID-19 Kidney Biopsy Consortium

Rebecca May[1], Clarissa Cassol[1], Andrew Hannoudi[1], Edgar Lerma[2], Christine Vanbeek[3], Mahesha Vankalakunti[4], Patrick Walker[1], T. David Bourne[1], Nidia Messias[1], Josephine Ambruzs[1], Christie Boils[1], Shree Sharma[1], L. Nicholas Cossey[1], Pravir Baxi[5], Chris Larsen[1], Matthew Palmer[6], Jonathan Zuckerman[7], Vighnesh Walavalkar[8], Anatoly Urisman[8], Roger Rodby[5], Valerie Luyckx[9], Juan Carlos Velez[10], Tiffany Caza[1]

[1]Arkana Laboratories, Little Rock, AR, [2]Advocate Christ Medical Center, Oak Lawn, IL, [3]AmeriPath/Quest Diagnostics, OK, [4]Manipal Hospital, Bangalore, India, [5]Rush University, Chicago, IL, [6]University of Pennsylvania, Philadelphia, PA, [7]University of California, Los Angeles, Los Angeles, CA, [8]University of California, San Francisco, San Francisco, CA, [9]University Hospital Zurich, Zurich, Switzerland, [10]Ochsner Health System, New Orleans, LA

Disclosures: Rebecca May: None; Andrew Hannoudi: None; Mahesha Vankalakunti: None; T. David Bourne: None; Nidia Messias: None; L. Nicholas Cossey: None; Pravir Baxi: None; Chris Larsen: None; Matthew Palmer: None; Vighnesh Walavalkar: None; Anatoly Urisman: None; Juan Carlos Velez: *Consultant*, Mallinckrodt Pharmaceuticals; *Speaker*, Otsuka Pharmaceuticals; *Advisory Board Member*, Retrophin; Tiffany Caza: None

Background: Acute kidney injury (AKI) is a frequent clinical finding in patients with COVID-19. Patients with AKI alone, with or without requirement for renal replacement therapy, have increased mortality. As the etiology of AKI in COVID-19 is largely unknown, an international collaborative group was established to provide clinicopathologic correlation through evaluation of a large number of kidney biopsies to understand the spectrum of kidney disease and outcomes in COVID-19 patients.

Design: Kidney biopsies from patients with confirmed COVID-19 received from 3/1/20-10/17/20 were included from multiple centers. A total of 102 kidney biopsies were evaluated, including 88 native and 14 allograft cases. Clinical information was provided from nephrologists for clinicopathologic correlation.

Results: The study population ranged from 10-77 years old (mean= 50 years) and consisted of 56% males and 44% females. There were more African American patients (49%) compared to patients of Caucasian, Hispanic, or Native American descent . The indication for biopsy was most often acute kidney injury (55%), followed by proteinuria (38%). The most common diagnosis in native biopsies was collapsing glomerulopathy (n=32), also known as COVID-19 associated nephropathy (COVAN), of which 97% were in African Americans. The remainder of biopsies had a variety of histopathologic diagnoses (Table 1). In the 14 transplant biopsies, the most common indication for biopsy was acute kidney injury (86%). In allografts, rejection was seen in 7 cases, with the other biopsies showing collapsing glomerulopathy (n=2), thrombotic microangiopathy (n=1), and IgA nephropathy (n=1). Immunohistochemistry for SARS-CoV-2 was performed in 54 cases (53%), all of which were negative. Clinical follow-up is ongoing.

	Number of Cases with Finding	Percentage of Cases with Finding
Native Biopsies (n=88)		
Collapsing Glomerulopathy	32	36.4%
Diabetic Nephropathy	15	14.7%
Arterionephrosclerosis	9	10.2%
Acute Tubular Injury	7	8.0%
Podocytopathies (primary, non-collapsing)	4	4.5%
FSGS (Secondary)	6	6.8%
Membranous Nephropathy PLA2R (n=1)	4	4.5%

NELL1 (n=1) Negative for PLA2R, NELL1, THSD7A, EXT1/2 (n=2)		
Pauci-Immune Crescentic Glomerulonephritis	4	4.5%
Amyloidosis	3	3.4%
Acute Interstitial Nephritis	3	3.4%
Infection Related Glomerulonephritis	3	3.4%
Thrombotic Microangiopathy	2	3.4%
Lupus Nephritis	2	2.3%
Myoglobin Cast Nephropathy	2	2.3%
Bile Cast Nephropathy	1	1.1%
IgA Nephropathy	1	1.1%
Fibrillary Glomerulopathy	1	1.1%
Allograft Biopsies (n=14)		
Transplant Rejection	7	50.0%
Collapsing Glomerulopathy	2	14.2%
Negative for Rejection (only diagnosis)	2	14.2%
Thrombotic Microangiopathy	1	7.1%
IgA Nephropathy	1	7.1%
Arterionephrosclerosis	1	7.1%

Table 1: Pathologic findings in kidney biopsies of COVID-19 patients (n=102).

Conclusions: A wide spectrum of kidney disease is seen in COVID-19 patients, supporting a role for kidney biopsy in this population. Collapsing glomerulopathy was the most frequent diagnosis in native biopsies, illustrating one contributor to the poor outcomes following COVID-19 infection seen in African Americans. Chronic disease was also seen in a high proportion of biopsies, supporting the notion that these patients may have less ability to handle the systemic stress of COVID-19.

843 Clinicopathologic Features of Non-Lupus Membranous Nephropathy in the Pediatric Population

Paul Miller[1], Li Lei[2], Vivek Charu[3], John Higgins[4], Richard Sibley[1], Megan Troxell[1], Neeraja Kambham[2]
[1]Stanford University Medical Center, Stanford, CA, [2]Stanford University, Stanford, CA, [3]Stanford Medicine/Stanford University, Stanford, CA, [4]Stanford University Hospital, Stanford, CA

Disclosures: Paul Miller: None; Li Lei: None; Vivek Charu: None; John Higgins: None; Richard Sibley: None; Megan Troxell: None; Neeraja Kambham: None

Background: Membranous nephropathy (MN) is an uncommon cause of nephrotic syndrome in children and can be categorized as either primary (intrinsic podocyte antigen) or secondary (planted antigens/immune complexes). Recent strides in understanding of primary MN have identified several podocyte proteins thought to represent autoantigenic targets. The two most common causes of secondary MN are hepatitis B infection (HBV) and systemic lupus erythematous (SLE).

Design: Renal biopsy files were searched (01/1995- 09/2020) for patients £ 20 yrs of age with MN, excluding those with SLE at/within 6 months of biopsy. All biopsies and clinical records were reviewed. Biopsy staining for PLA2R {immunofluorescence (IF) or immunohistochemistry (IHC) based on tissue availability}, NELL-1 (IHC) and IgG subtypes (IF) was performed.

Results: Forty-one patients, including 16 children (<12 yrs of age) and 25 adolescents (13-20 yrs), were identified. At presentation, all patients had proteinuria, 26 had nephrotic syndrome, and 25 had hematuria. On biopsy, 16 had mesangial proliferation, 38 had <20% interstitial fibrosis and tubular atrophy (IFTA), and 3 had >50% IFTA. None showed "full house" staining and 1 had ≥1+C1q staining (see Table 1). Fourteen patients (34%), including 4 children (25%) and 10 adolescents (40%), had positive biopsy staining for PLA2R and 1 adolescent had positive

staining for NELL-1. IgG4 dominance was seen in both PLA2R+ (57%) and PLA2R- (44%) cases. Serum PLA2R was negative in 3 biopsy PLA2R- patients. Co-morbidities included 4 patients diagnosed with MN during pregnancy (10-26 wks gestation), 3 with remote or current HBV infection, and 1 each with IPEX syndrome, Von Hippel Lindau syndrome, Down syndrome, and lysunuric protein intolerance. Two seronegative (ANA- and anti-dsDNA-), biopsy PLA2R- patients manifested clinical SLE 4 and 9 years post biopsy. Of patients with follow-up data (28 patients, mean 65 mo follow-up), 10 experienced complete (1 spontaneous), and 7 partial remission; 9 patients had no treatment response, including 3 who progressed to ESKD and had a kidney transplant. Two of the transplanted patients suffered disease recurrence.

	Total cases (N=41)	Children (N=16)	Adolescents (N=25)
F:M ratio	22:19	8:8	14:11
+ ANA (ds-DNA-, normal C3, C4)*	3	1	2
Low C3 or C4	2	0	2
Hematuria	25 (61%)	11 (69%)	14 (56%)
Prior Immunosuppresants	11 (27%)	6 (38%)	5 (20%)
Mesangial/subendothelial deposits	12 (29%)	6 (38%)	6 (24%)
Tubuloreticular inclusions	6 (15%)	3 (19%)	3 (12%)
PLA2R+	14 (34%)	4 (25%)	10 (40%)
NELL-1+	1	0	1

*did not develop SLE (mean 11 year follow up)

Conclusions: Our non-lupus MN study represents one of the largest pediatric cohorts reported to date. Despite excluding lupus MN (typically PLA2R-), PLA2R positivity in our patients (34%) is significantly lower than reported in the adults (~60%). Furthermore, children showed less PLA2R positivity (25%) than adolescents (40%). Only 6 patients (15%) had identifiable non-lupus cause of secondary MN. These findings suggest that etiology of pediatric MN is multifactorial with an unclear cause in a significant proportion.

844 Systems-Based Analysis of the Transcriptome of IgA Nephropathy

Kenneth Ofori[1], Amin Yakubu[2], Alex Rai[3]
[1]Columbia University Medical Center, New York, NY, [2]Genesis Research, Hoboken, NJ, [3]Columbia University Irving Medical Center, New York-Presbyterian Hospital, New York, NY

Disclosures: Kenneth Ofori: None; Amin Yakubu: None; Alex Rai: None

Background: IgA nephropathy (IgAN) is the most common primary glomerulonephritis. It is characterized by mesangial deposition of immune complexes consisting of aberrantly glycosylated IgA, resulting in complement activation, mesangial proliferation and matrix synthesis, cytokine release, immune cell infiltration and tubulointerstitial injury. There is currently no IgAN specific therapy and about 30-40%of patients develop ESRD in 20-30 years.

Systems approaches to analysis of transcriptomic data is a powerful tool in elucidating disease mechanisms and identifying drug targets. We holistically evaluate the IgAN transcriptome, involving differential gene expression (DGE) with a co-expression based functional analyses of the differentially expressed genes (DEGs), modular co-expression analyses, differential gene correlation and characterization of immune signatures.

Design: Affymetrix microarray files from GSE93798 from glomeruli of 20 IgAN samples and 22 healthy controls were downloaded using GEOquery. DGE was performed with Limma, using adjusted p-value of 0.01 and a fold change of 2 as threshold. KEGG analysis of DEGs was done with COGENA. Module identification and differential enrichment, and KEGG pathway analysis of modules was performed with CEMiTools.

Differential gene correlation was done using DGCA. Functional analysis of differentially correlated genes was done with cytoscape.

Immune signature enrichment was determined using imsig.

Results: 174 genes were upregulated and 349 were downregulated in IgAN. Functional analysis after clustering into 7 groups revealed upregulation of known pathways involved in IgAN including focal adhesion, complement and coagulation cascades, and extracellular matrix receptor interaction. Cluster 6, a group of co-repressed downregulated genes, showed enrichment for multiple amino acid metabolic pathways.

Six modules of co-expressed genes were identified, 3 of which showed significant pathway enrichment. Module 1, enriched in various amino acid metabolism pathways, was repressed in IgAN. Modules 2 and 6, enriched in focal adhesion, antigen processing, cytokine-cytokine receptor interaction and intestinal immune network for IgA production, NK- cell mediated cytotoxicity and FC-gamma receptor mediated phagocytosis, were upregulated in IgAN.

232 genes had significantly different change in average correlation. These genes were enriched in metabolic and immune processes.

Immune cells and interferon, translation and proliferation signatures were enriched in IgAN.

Figure 1 - 844

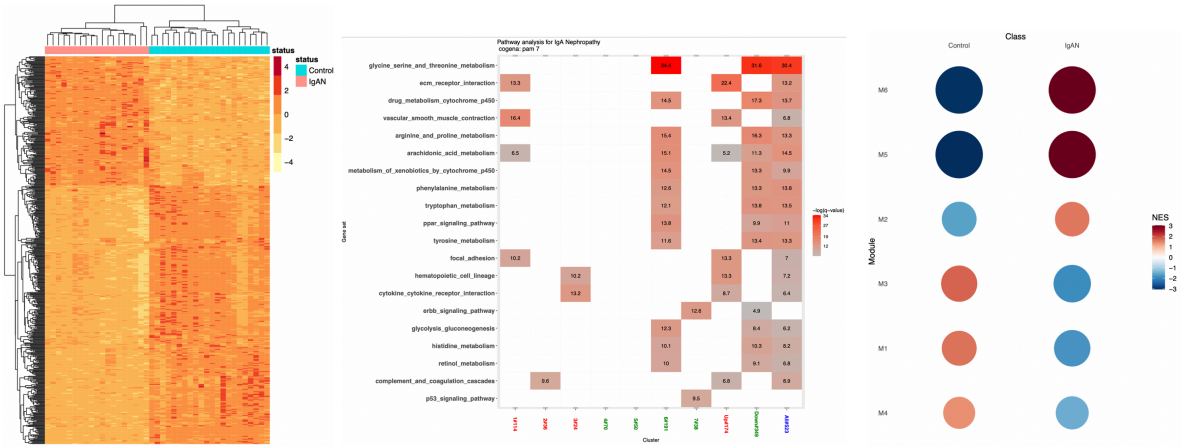

(1a) Heatmap of differentially expressed genes

(1b) KEGG pathway enrichment of DEGs after clustering into 7 co-expressed groups. Red labeled groups are upregulated clusters and green labeled ones are downregulated clusters

(1c) Modules identification and enrichment

Figure 2 - 844

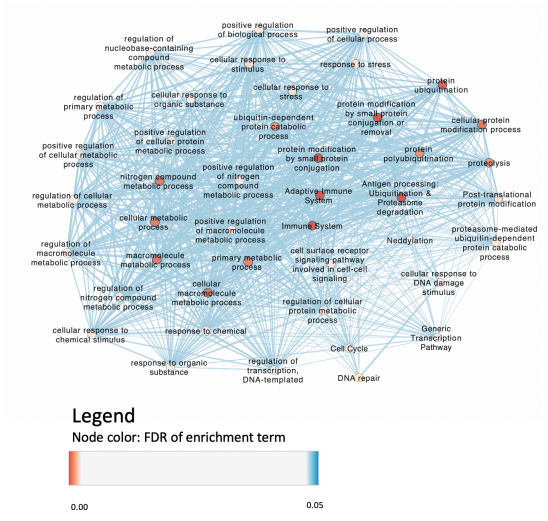

(2a) Enrichment map of differentially correlated genes

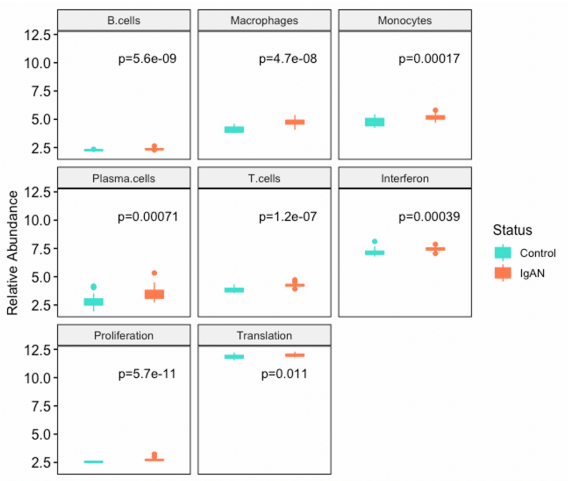

(2b) Immune cell and immune signatures enrichment

Conclusions: Systems approaches identified known pathways and immune signatures involved in IgAN. Additionally, repression of amino acid metabolism was found. Modulation of amino acid metabolism may be a therapeutic option in IgAN. Targeting interferon, translation and/or proliferation signatures may also be useful in IgAN.

845 Survey on the Pathologic Evaluation of Non-Neoplastic Kidney in Kidney Cancer Specimens

James Paik[1], Carla Ellis[2], Kammi Henriksen[1], Anthony Chang[1]
[1]University of Chicago, Chicago, IL, [2]Feinberg School of Medicine/Northwestern University, Chicago, IL

Disclosures: James Paik: None; Kammi Henriksen: None; Anthony Chang: None

Background: Medical renal diseases can occur in up to 60% of kidney tumor resection specimens, and their diagnoses and treatment are as important as the emerging goal of renal function preservation in kidney cancer therapy. The evaluation of the non-neoplastic kidney has been a required parameter for kidney cancers using the College of American Pathologists (CAP) synoptic reports since 2010, but the impact of this implementation on the practice behavior of pathologists is unknown. We conducted this survey of genitourinary (GU) and renal pathologists to assess the current approach regarding this specific aspect of tumor resection specimens.

Design: We emailed a 14-item multiple-choice survey to members of the Renal Pathology Society and Genitourinary Pathology Society. Data were collected via RedCap. Analysis was performed, and p-values were generated using two-proportion Z-tests.

Results: Of the 202 respondents, 96 (48%) practiced in the United States. 104 identified as renal pathologists, and 98 identified as GU pathologists. The vast majority of tumor resection specimens are evaluated by GU pathologists. 89 (92%) GU and 96 (98%) renal pathologists report evaluating the non-neoplastic tissue of tumor nephrectomies. When specimens are processed, 58% automatically apply special stains (Jones, PAS, Mason trichrome, etc.) to the tissue, a minority automatically order immunofluorescence and electron microscopy, and 29% only assess H&E stained slides. 71% use synoptic reporting; of these, 84% use protocols that require non-neoplastic evaluation of the parenchyma, and 81% use the CAP protocol. Between the two specialties, 36% of GU and 42% of renal pathologists always alert urologists when they find evidence of medical renal disease (P=0.39). 22% of GU pathologists and 9% of renal pathologists never alert urologists (P=0.02).

Conclusions: Most kidney tumor resection specimens are evaluated by GU pathologists. The vast majority of renal and GU pathologists examine non-neoplastic areas of tumor nephrectomy specimens as required by their synoptic reporting protocols, but this survey cannot determine the quality of this evaluation. There are some differences regarding the evaluation and communication with clinicians between GU and renal pathologists. For example, renal pathologists are more likely to communicate the diagnoses directly with the treating physician despite being less frequent evaluators. These data provide opportunities for future advocacy and education on this important yet overlooked topic.

846 Renal Light Chain Deposition Disease Concurrent with AL Amyloidosis: A Report of 14 Cases

Samar Said[1], Alejandro Best Rocha[2], Surendra Dasari[1], Jason Theis[1], Nelson Leung[3], Mariam Priya Alexander[1], Ellen McPhail[1], Samih Nasr[1]
[1]Mayo Clinic, Rochester, MN, [2]Arkana Laboratories, Little Rock, AR, [3]Mayo Clinic Foundation, Rochester, MN

Disclosures: Samar Said: None; Alejandro Best Rocha: None; Surendra Dasari: None; Jason Theis: None; Nelson Leung: *Consultant*, AbbVie; Mariam Priya Alexander: None; Ellen McPhail: None; Samih Nasr: None

Background: The pattern of kidney injury due to monoclonal gammopathy is determined by the structural and physiologic properties of the abnormal immunoglobulin light chain (LC). AL amyloidosis and light chain deposition disease (LCDD) are the 2 most common glomerulopathies secondary to monoclonal LCs, but the occurrence of

both lesions in the same kidney biopsy is extremely rare. Here, we report the first series of LCDD concomitant with AL (LCDD+AL).

Design: 14 patients with LCDD+AL were identified by retrospective review of all native kidney biopsies processed in our Renal Biopsy Laboratory from 1993-2020. The clinical, pathologic, molecular, and outcome characteristics were reviewed.

Results: Patients were 79% females, 92% White, with a median age of 66 years, who presented with proteinuria (100%), hematuria (86%), renal insufficiency (93%) and nephrotic syndrome (38%). Extrarenal involvement was present in 38% (of liver in 23% and of heart in 23%). The hematologic condition was symptomatic myeloma in 57% and MGRS in 43%. No patient had biclonal gammopathy. Histologically, all cases showed Congo red positive fibrillar amyloid deposits that stained for 1 LC on IF (κ in 50%) which involved vessels (86%), glomeruli (57%), and interstitium (29%), as well as concurrent LCDD with diffuse linear staining of GBM and TBM for 1 LC (same isotype as the amyloidogenic LC) with corresponding non-fibrillar punctate electron dense deposits ultrastructurally. AL was restricted to vessels in 42%. The LC variable domain gene, determined by proteomic analysis of amyloid deposits in 6, was LV2-11 in 2, LV2-14 in 1, KV1-5 in 1, KV3-15 in 1, and KV4-1 in 1. Plasma cell gene sequencing in 1 identified a single dominant clone (VK1 L12). On follow up (median 19 months), 8 (57%) progressed to ESRD and 7 (50%) died; overall, 12 (86%) progressed to ESRD and/or died. Chemotherapy was given to 12. The 2 with renal and overall survival were among the 7 who received bortezomab-based therapy.

Conclusions: LCDD+AL mainly affects elderly females, is associated with symptomatic myeloma in >half of patients, is not associated with a certain LC isotype or variable region gene family, and has poor renal and overall survival. This report adds to the complexity of pathophysiology of LC glomerulopathies.

847 Cortical Tubulointerstitial Mononuclear Inflammation in Renal Biopsies is a Quantitative Biomarker of Clinical Outcomes in NEPTUNE Glomerular Diseases

Gina Sotolongo[1], Jihyeon Je[2], Jarcy Zee[3], Yijiang Chen[4], Xiang Li[2], Yuqi Wang[2], Jeffrey Hodgin[5], Anant Madabhushi[4], Andrew Janowczyk[4], Kyle Lafata[2], Laura Barisoni[2]
[1]Duke University Health System, Durham, NC, [2]Duke University, Durham, NC, [3]The Children's Hospital of Philadelphia, Perelman School of Medicine at the University of Pennsylvania, Philadelphia, PA, [4]Case Western Reserve University, Cleveland, OH, [5]University of Michigan, Ann Arbor, MI

Disclosures: Gina Sotolongo: None; Jihyeon Je: None; Jarcy Zee: None; Yijiang Chen: None; Xiang Li: None; Yuqi Wang: None; Jeffrey Hodgin: None; Anant Madabhushi: *Consultant*, Aiforia Inc; *Primary Investigator*, Bristol Myers-Squibb; *Primary Investigator*, Astrazeneca; *Primary Investigator*, Boehringer-Ingelheim; Andrew Janowczyk: None; Kyle Lafata: None; Laura Barisoni: None

Background: Tubulointerstitial changes assessed in glomerular diseases, such as tubular atrophy and interstitial fibrosis or inflammation, are known to associate with clinical outcomes. In current clinical practice, the amount of inflammation in native and transplant renal biopsies is conventionally reported using a semiquantitative scale. This approach, however, does not provide an accurate quantitative measure of the exact amount of inflammatory cells. Additionally, human assessment in general has limited reproducibility. This study aims to a) establish a protocol for efficient semi-automatic detection and quantification of cortical mononuclear inflammation in kidney biopsies via a quantitative pathology software tool (QuPath), and b) investigate the association of quantifiable inflammation with clinical outcomes.

Design: The Nephrotic Syndrome Study Network (NEPTUNE) Hematoxylin & Eosin (H&E) whole slide image (WSI) dataset was first curated using HistoQC. Subsequently, a diverse set of 47 good quality WSIs from patients with glomerular diseases was selected. QuPath's cell-detector algorithm was employed to segment all cells in each WSI by first manually annotating (segmenting) ≥100 mononuclear inflammatory and 300 non-inflammatory nuclei in the renal cortex per each biopsy. These manual annotations were then used to train a random trees cell classifier to identify mononuclear inflammatory and non-inflammatory cells. The classifier was iteratively refined via manual corrections until an optimal classification result was achieved (Fig. 1).

The renal cortex of each biopsy was also manually segmented to calculate the ratio between cortical inflammatory and non-inflammatory cortical cells. Kaplan-Meier analysis was used to test the association between the amount of mononuclear inflammatory cells and clinical outcome (time to 40% eGFR decline or kidney replacement).

Results: Across the 47 WSIs, the median cortical inflammatory cell ratio was 0.06, ranging from 0.00 to 0.32. Kaplan-Meier curves and a log-rank test comparing high inflammation (>0.6) and low inflammation (≤0.6) show that high levels of mononuclear inflammation are associated with worse disease progression (p=0.043) (Fig. 2).

Figure 1 - 847

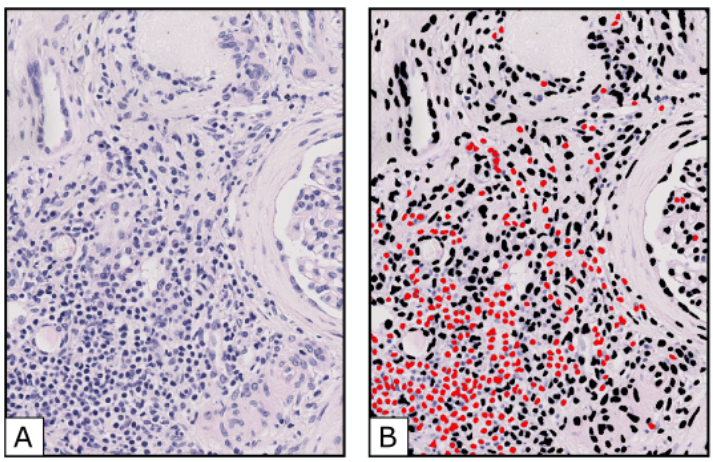

A) Original WSI B) After applying classifier

Figure 2 - 847

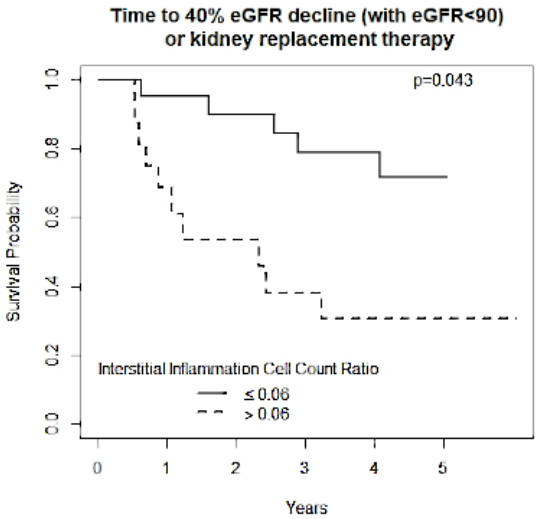

Conclusions: These preliminary studies show that image analysis tools, such as QuPath, provide an efficient quantifiable measure of cortical mononuclear inflammation that can be used as a biomarker of clinical outcomes in glomerular diseases.